Cellular/Molecular

# mGluR Control of Interneuron Output Regulates Feedforward Tonic GABA$_A$ Inhibition in the Visual Thalamus

**Adam C. Errington,**[1] **Giuseppe Di Giovanni,**[1,2] **Vincenzo Crunelli,**[1] **and David W. Cope**[1]
[1]Neuroscience Division, School of Biosciences, Cardiff University, Cardiff CF10 3AX, United Kingdom, and [2]Department of Physiology and Biochemistry, Faculty of Medicine and Surgery, University of Malta, Msida MSD 2080, Malta

Metabotropic glutamate receptors (mGluRs) play a crucial role in regulation of phasic inhibition within the visual thalamus. Here we demonstrate that mGluR-dependent modulation of interneuron GABA release results in dynamic changes in extrasynaptic GABA$_A$ receptor (eGABA$_A$R)-dependent tonic inhibition in thalamocortical (TC) neurons of the rat dorsal lateral geniculate nucleus (dLGN). Application of the group I selective mGluR agonist dihydroxyphenylglycine produces a concentration-dependent enhancement of both IPSC frequency and tonic GABA$_A$ current (I$_{GABA}$tonic) that is due to activation of both mGluR1a and mGluR5 subtypes. In contrast, group II/III mGluR activation decreases both IPSC frequency and I$_{GABA}$tonic amplitude. Using knock-out mice, we show that the mGluR-dependent modulation of I$_{GABA}$tonic is dependent upon expression of δ-subunit containing eGABA$_A$Rs. Furthermore, unlike the dLGN, no mGluR-dependent modulation of I$_{GABA}$tonic is present in TC neurons of the somatosensory ventrobasal thalamus, which lacks GABAergic interneurons. In the dLGN, enhancement of IPSC frequency and I$_{GABA}$tonic by group I mGluRs is not action potential dependent, being insensitive to TTX, but is abolished by the L-type Ca$^{2+}$ channel blocker nimodipine. These results indicate selective mGluR-dependent modulation of dendrodendritic GABA release from F2-type terminals on interneuron dendrites and demonstrate for the first time the presence of eGABA$_A$Rs on TC neuron dendritic elements that participate in "triadic" circuitry within the dLGN. These findings present a plausible novel mechanism for visual contrast gain at the thalamic level and shed new light upon the potential role of glial ensheathment of synaptic triads within the dLGN.

## Introduction

GABAergic interneurons play a critical role in the dynamic regulation of information transfer through primary sensory thalamic nuclei. In the dorsal lateral geniculate nucleus (dLGN), interneurons can alter the temporal precision of retinogeniculate inputs (Blitz and Regehr, 2005; Crunelli et al., 1988), the receptive field properties of thalamocortical (TC) neurons, the principal projection neurons of the thalamus (Sillito and Kemp, 1983; Berardi and Morrone, 1984; Holdefer et al., 1989), and dynamically sculpt thalamic network activity (Lorincz et al., 2009). Interneurons innervate TC neurons via conventional axodendritic synapses, or F1 terminals, and dendrodendritic synapses, or F2 terminals, that partake in specialized synaptic "triads" where the interneuron dendrite is postsynaptic to retinogeniculate terminals and presynaptic to the TC neuron dendrite (Famiglietti and Peters, 1972; Grossman et al., 1973; Ohara et al., 1983; Hamos et

al., 1985). GABA release from the two terminals differs in its action potential dependence, F1 and F2 terminals being action potential dependent and action potential independent, respectively (Cox and Sherman, 2000; Govindaiah and Cox, 2006), and F2 terminals express both ionotropic and metabotropic glutamate receptors (mGluRs) (Godwin et al., 1996; Cox and Sherman, 2000). Glutamate release from retinogeniculate terminals can therefore monosynaptically excite TC neuron dendrites and disynaptically inhibit them via glutamate receptor-dependent GABA release from F2 terminals (Cox and Sherman, 2000; Govindaiah and Cox, 2004, 2006; Blitz and Regehr, 2005). However, the functional roles of F2 terminals are not completely understood, but may rely on their ability to release GABA independent of somatic activity (Cox et al., 1998; Cox and Sherman, 2000; Govindaiah and Cox, 2006).

GABA release from interneurons activates synaptic GABA$_A$ receptors (GABA$_A$Rs) to generate "phasic" inhibition (i.e., classical IPSCs). More recently, a persistent GABA$_A$R-mediated "tonic" inhibition that is generated by extrasynaptic GABA$_A$Rs (eGABA$_A$Rs) has been demonstrated in TC neurons of the dLGN and the somatosensory ventrobasal (VB) thalamus (Belelli et al., 2005; Cope et al., 2005, 2009; Jia et al., 2005; Bright et al., 2007), a nucleus devoid of interneurons (Barbaresi et al., 1986; Harris and Hendrickson, 1987). Tonic GABA$_A$ currents (I$_{GABA}$tonics) have important physiological and pathophysiological roles in the thalamus (Cope et al., 2005, 2009; Bright et al., 2007), and are gener-

**Table 1. IPSC properties in TC neurons under control conditions**

| | | IPSC parameter | | | | |
|---|---|---|---|---|---|---|
| | $n$ | Peak amplitude (pA) | Weighted decay (ms) | Frequency (Hz) | Charge (fC) | Total current (pA) |
| dLGN (pre-bath- applied DHPG) | 9 | −40.4 ± 2.7 | 2.6 ± 0.2 | 6.9 ± 2.4 | −122.1 ± 15.7 | −0.9 ± 0.3 |
| dLGN (control population) | 14 | −42.3 ± 2.0 | 3.0 ± 0.2 | 9.7 ± 1.4 | −139.4 ± 8.1 | −1.4 ± 0.3 |
| VB thalamus | 9 | −47.0 ± 6.1 | 2.4 ± 0.3 | 6.8 ± 0.7 | −136.5 ± 30.7 | −1.0 ± 0.3 |

Data are presented as mean ± SEM. Number of recorded neurons ($n$) are as indicated.

ated, at least in part, by the spillover of neurotransmitter from the synaptic cleft following conventional vesicular GABA release (Bright et al., 2007). Modulating vesicular GABA release may therefore influence tonic as well as phasic GABA$_A$ inhibition (Bright and Brickley, 2008). Since mGluR activation modulates GABA release from both F1 and F2 terminals (Cox and Sherman, 2000; Govindaiah and Cox, 2004, 2006), we have here examined the effect of mGluR activation on tonic GABA$_A$ inhibition. Our data show that mGluRs control tonic inhibition in TC neurons of the dLGN, but not VB thalamus, almost exclusively by modulating GABA release from F2 terminals in an L-type Ca$^{2+}$ channel- dependent manner, indicating that eGABA$_A$Rs may play a previously unappreciated role in modulating sensory information processing in the visual thalamus.

## Materials and Methods

*Electrophysiology.* Coronal slices (300 $\mu$m) containing the dLGN or horizontal slices containing the VB thalamus and the thalamic reticular nucleus (NRT) were prepared from postnatal day 20 (P20) to P25 Wistar rats of either sex in chilled (1–3°C) cutting solution bubbled with carbogen (95% O$_2$/5% CO$_2$) (in mM: 60 sucrose, 85 NaCl, 2.5 KCl, 1 CaCl$_2$, 2 MgCl$_2$, 1.25 NaH$_2$PO$_4$, 25 NaHCO$_3$, 25 D-glucose, 3 kynurenic acid, 0.045 indomethacin) in accordance with the Home Office Animals (Scientific Procedures) Act 1986, United Kingdom. For experiments in $\delta$-subunit knock-out mice ($\delta^{-/-}$), coronal slices including the dLGN were prepared from postnatal day 21–24 $\delta^{-/-}$ mice or wild-type (WT) littermates. Slices were stored for 20 min at 35°C in sucrose containing solution and then maintained at room temperature in artificial CSF (aCSF) (in mM: 125 NaCl, 2.5 KCl, 1 CaCl$_2$, 2 MgCl$_2$, 1.25 NaH$_2$PO$_4$, 25 NaHCO$_3$, 25 D-glucose, 305 mOsm) and used within 4–6 h. For recording, slices were transferred to a submersion chamber continuously perfused with warmed (33–34°C) aCSF (in mM: 125 NaCl, 2.5 KCl, 2 CaCl$_2$, 1 MgCl$_2$, 1.25 NaH$_2$PO$_4$, 25 NaHCO$_3$, 25 D-glucose, 305 mOsm) at a flow rate of 2–2.5 ml/min. For voltage-clamp recordings of IPSCs and I$_{GABA}$tonic, 3 mM kynurenic acid was added to the solution to block ionotropic glutamate receptors and isolate GABAergic currents. Somatic whole-cell voltage-clamp recordings were performed on TC neurons (visually identified by infrared videomicroscopy) using pipettes with resistances of 2–5 M$\Omega$ when filled with internal solution containing the following (in mM): 130 CsCl, 2 MgCl$_2$, 4 Mg-ATP, 0.3 Na-GTP, 10 Na-HEPES, 0.1 EGTA, pH 7.3, 290–295 mOsm. All experiments were performed at a holding voltage (V$_h$) of −70 mV unless specifically indicated otherwise. For current-clamp recordings of NRT neurons, an internal solution containing (in mM) 140 K$^+$-gluconate, 4 Na$_2$ATP, 0.1 CaCl$_2$, 5 MgCl$_2$, 1 EGTA, 10 HEPES, 15 Na$^+$-phosphocreatine, pH 7.3, and 290–295 mOsm was used. For anatomical identification of NRT neurons, internal patch solution was supplemented with 1% biocytin and *post*
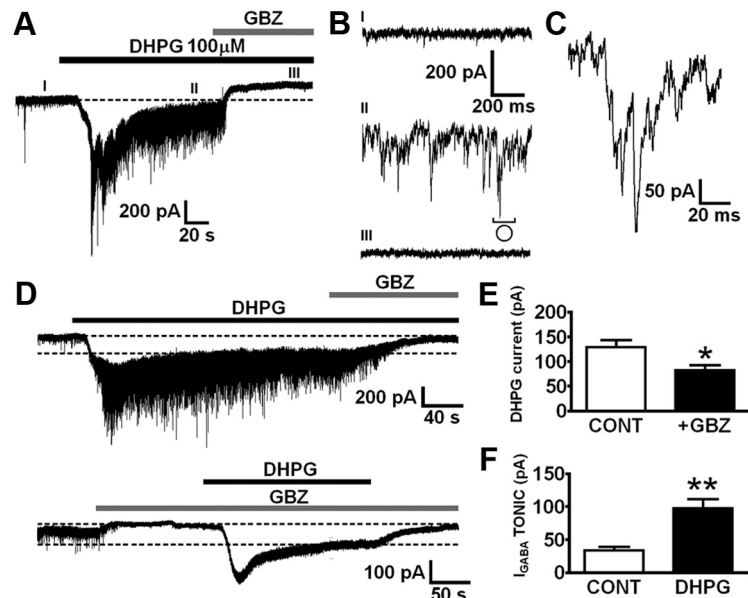


**Figure 1.** Activation of group I mGluRs increases tonic GABA$_A$ inhibition in TC neurons of the dLGN. **A**, Representative current trace from a dLGN TC neuron showing that bath application of the group I mGluR selective agonist DHPG (100 $\mu$M, black bar) causes an inward shift in holding current that is blocked by focal application of GBZ (100 $\mu$M, gray bar). GBZ not only blocks the DHPG-induced inward current, but also reveals the presence of a tonic GABA$_A$ current compared with control conditions (dashed line). **B**, Expanded current traces from the same neuron as in **A** showing the increase in IPSC frequency caused by application of DHPG (**BII**) compared with control (**BI**) and the block of spontaneous synaptic currents by GBZ (**BIII**). Note the occurrence of IPSC bursts in the presence of DHPG (open circle). **C**, Current trace depicting the IPSC burst identified by the asterisk in **B**. **D**, Application of DHPG to dLGN neurons (black bar) produces an inward shift in holding current, a proportion of which is mediated by increased I$_{GABA}$tonic, as revealed by application of GBZ (gray bar). Application of DHPG in the continuous presence of GBZ (bottom) reveals the presence of a non-GABA$_A$-dependent I$_{DHPG}$. Dashed lines represent the mean control holding current and the DHPG-induced plateau current. **E**, Summary of the decrease in DHPG-induced inward current in the presence of GBZ. **F**, Summary of the increase in I$_{GABA}$tonic in the presence of DHPG. *$p < 0.05$, **$p < 0.01$.

*hoc* histochemical procedures were performed as previously described (Williams et al., 1996). Electrophysiological data were acquired at 20 kHz and filtered at 6 kHz using a Multiclamp 700B patch-clamp amplifier and pClamp 9.0/10.0 software (Molecular Devices). Series resistance at the start of experiments was between 11 and 15 M$\Omega$, was compensated by ~80%, and varied ≤ 30% during recordings. The presence of I$_{GABA}$tonic was determined following the focal application of 100 $\mu$M 6-imino-3-(4-methoxyphenyl)-1(6$H$)-pyridazinebutanoic acid hydrobromide [gabazine (GBZ)] as previously described (Cope et al., 2005). All other drugs were bath applied.

For synaptic stimulation experiments, an angled slice preparation was used to maintain intact retinal ganglion cell (RGC) input to the dLGN. Briefly, a tissue block was prepared by performing two cuts angled at 45° to the midline to preserve the optic tract running from the optic chiasm to the LGN of one hemisphere. Typically, two 300 $\mu$m slices could be obtained from each brain with demonstrable synaptic connectivity. Stimulation was achieved by placing a bipolar tungsten electrode (Frederick Haer) into the optic tract before it entered the ventral LGN (vLGN) (compare Fig. 7$A$) and delivering pulses of 200 $\mu$s duration with intensities between 10 and 300 $\mu$A. Tetanic stimulation was achieved using a train of 40 pulses delivered at 200 Hz (total stimulus duration 200 ms).

*Data analysis.* Data were filtered off-line at 3 kHz and analyzed using LabView-based software, as described previously (Cope et al., 2005, 2009). To determine the effect of (RS)-3,5-dihydroxyphenylglycine
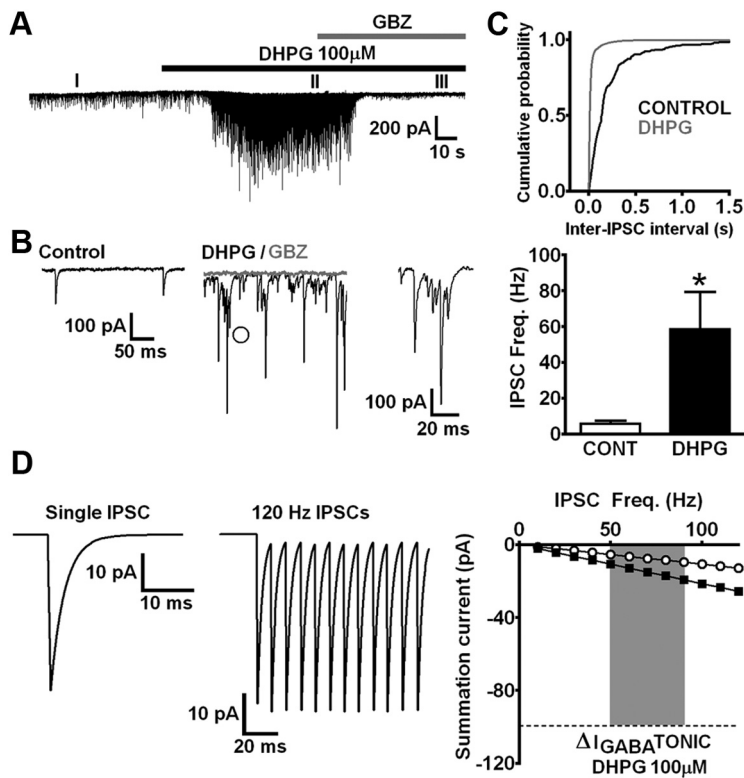
**Figure 2.** IPSC summation does not account for the inward current shift evoked by mGluR activation. **A**, A typical trace showing a recording made from a vLGN neuron under our standard recording conditions. DHPG (100 μM) application (black bar) produced a significant increase in IPSC frequency without inducing a persistent inward current. Application of GBZ (gray bar) revealed a lack of I$_{GABA}$tonic in these neurons as has been shown previously. **B**, Expanded traces showing the regions labeled I, II, and III in **A**, respectively. In the presence of GBZ (gray trace overlaid) IPSCs are completely blocked without any change in holding current. Note the presence of IPSC bursts (indicated by open circle and expanded further right) in these vLGN neurons that are comparable to those observed in dLGN and the relative lack of baseline "noise" in the absence of I$_{GABA}$tonic. **C**, The cumulative probability distribution for the cell depicted in **A** shows a significant ( $p < 0.001$) left shift in inter-IPSC interval in the presence of DHPG (control black line, $n = 302$ events from 4 cells; DHPG gray line, $n = 1852$ events from 4 cells). Summary of the increase in IPSC frequency in four vLGN neurons. **D**, A simple model assuming linear summation shows that even high-frequency IPSCs do not summate sufficiently to produce large steady-state inward currents. White circles: IPSC amplitude − 41 pA, $\tau_W$ 2.6 ms; black squares: IPSC amplitude 82 pA, $\tau_W$ 2.6 ms. The shaded gray area illustrates the increase in tonic current produced by 100 μM DHPG (see Fig. 3C). *$p < 0.05$.

(DHPG) "wash-on" on baseline current, 10 s periods of current were measured before and after DHPG application. Epochs of 5 ms duration were sampled every 100 ms during these 10 s periods, and those that fell on IPSCs were discarded. The average baseline current was then calculated from the remaining epochs, and the difference between pre- and post-DHPG application determined. To measure tonic currents in different populations of neurons, the average baseline current was calculated as above for three 10 s periods, two before focal application of GBZ (1 and 2), and one after (3). I$_{GABA}$tonic was deemed to be present for a given neuron if the GBZ-dependent "shift" (i.e., 3–2) was twice the SD of the background "drift" (i.e., 2–1) (Cope et al., 2005). The average I$_{GABA}$-tonic for a given experimental condition was then calculated, and the effects of drugs were compared in different populations. In some instances, tonic current amplitude was normalized to whole-cell capacitance, measured by small (5 mV) voltage pulses. For analysis of IPSCs before wash-on of DHPG, and in a control populations of neurons, individual IPSCs were averaged, and the peak amplitude, charge transfer (the integral of the average IPSC), weighted decay time constant [$\tau_W$ (integral divided by peak amplitude)], frequency, and total current (charge transfer × frequency) were measured. In the presence of DHPG, insufficient numbers of isolated IPSCs could be resolved to obtain reliable measurements of amplitude or $\tau_W$; therefore, only data on frequency are presented following drug applications. IPSC bursts were identified manually in pClamp 9.0/10.0, and the mean peak-to-peak interval was calculated from 30 consecutive bursts for each neuron. The population mean was then determined for each experimental condition. For

synaptic stimulation experiments, IPSC frequency and holding current were measured and binned at 1 s intervals. The I$_{GABA}$tonic was calculated by subtracting the stimulus-evoked response in the presence of GBZ from control responses. The effect of mGluR antagonists on evoked responses was determined by measuring the mean holding current in a 5 s bin after the end of the stimulus.

Tonic current amplitude, IPSC frequency and IPSC burst interval were compared under different experimental conditions using Student's unpaired $t$ test or one-way ANOVA with Bonferroni *post hoc* test, as appropriate. Inter-IPSC interval distributions were compared using the Kolmogorov–Smirnov test. Correlations between tonic current amplitude and IPSC frequency were determined using Pearson's test. Significance in all cases was set at $p < 0.05$. Data are expressed as mean ± SEM throughout.

*Sources of drugs.* Drugs were obtained from the following sources: DHPG, tetrodotoxin (TTX), ($S$)-(+)-α-amino-4-carboxy-2-methyl-benzeneacetic acid (LY367385), 1,4-dihydro-2,6-dimethyl-4-(3-nitrophenyl)-3,5-pyridinedicarboxylic acid 2-methyloxyethyl 1-methylethyl ester (nimodipine), and GBZ are from Tocris Bioscience; 3-((2-methyl-1,3-thiazol-4 yl) ethynyl)pyridine (MTEP), (1$S$,2$S$,5$R$,6$S$)-2-aminobicyclo[3.1.0]hexane-2,6-dicarboxylic acid (LY354740), L-(+)-2-amino-4-phosphonobutyric acid (L-AP4), 6-cyano-7-nitroquinoxaline-2,3-dione (CNQX), and D-(-)-2-Amino-5-phospho-nopentanoic acid (D-AP5) are from Ascent Scientific. Nimodipine was dissolved in DMSO, and LY354740 in equimolar NaOH, before addition to the aCSF.

## Results

### Activation of group I mGluRs increases tonic inhibition in TC neurons of the dLGN

Application of the group I-specific mGluR agonist DHPG increases vesicular GABA release from thalamic interneurons, resulting in augmented phasic GABA$_A$ inhibition in TC neurons of the dLGN (Govindaiah and Cox, 2006). Therefore, we bath applied DHPG (100 μM) to TC neurons in slices of rat brain maintained *in vitro* to test whether increased vesicular GABA release also enhanced eGABA$_A$Rs activation and I$_{GABA}$tonic. In whole-cell patch-clamp recordings (V$_h$: − 70 mV) under control conditions [i.e., in the presence of kynurenic acid (3 mM)] to block ionotropic glutamate receptors, baseline current was −209.3 ± 18.2 pA ($n = 9$), and the properties of spontaneous IPSCs were similar to those described previously (Cope et al., 2005; Bright et al., 2007) (Table 1). In all neurons tested, DHPG caused an inward shift in holding current that reached a plateau 1–2 min after commencing DHPG application (Fig. 1A). At the plateau, baseline current values were significantly more negative than under control conditions (−326.5 ± 26.1 pA, $p < 0.001$, Student's paired $t$ test), indicating a total inward shift of 117.2 ± 10.8 pA. Furthermore, DHPG application resulted in an increased IPSC frequency (from 6.9 ± 2.4 to 76.3 ± 10.1 Hz) that was reflected by a leftward shift in the distribution of inter-IPSC intervals ( $p < 0.001$, Kolmogorov–Smirnov test). Noticeably, in all neurons tested discrete IPSC clusters or bursts were regularly observed, and these had mean peak-to-peak intervals of 204.3 ± 6.7 ms (Fig. 1*BII,C*). To test whether the DHPG-

induced inward current was due to the activation of eGABA_ARs, we focally applied the GABA_AR antagonist GBZ (100 $\mu$M). Application of GBZ, in the continuing presence of DHPG, not only blocked all spontaneous IPSCs but also caused an outward shift in holding current, revealing the presence of I_GABAtonic (Fig. 1A). Since mGluR activation has multiple postsynaptic effects in TC neurons (McCormick and von Krosigk, 1992; Hughes et al., 2002), it is possible that part of the DHPG-induced inward current may have been caused by the activation of other cellular mechanisms in addition to eGABA_AR activation. To test this hypothesis, we compared currents evoked by DHPG in the presence and absence of GBZ. In a separate group of dLGN TC neurons, we found that DHPG produced an inward current of 129 ± 14.6 pA at plateau level, which was significantly larger ( $p < 0.05$, unpaired $t$ test, $n = 6$) (Fig. 1D,E) than that evoked in another group of neurons previously perfused with 100 $\mu$M GBZ (83.3 ± 9.9 pA, $n = 6$), a difference of 46. 3 ± 11.6 pA (Fig. 1E). This indicated that a fraction of the DHPG-induced inward current in TC neurons resulted from activation of a GBZ-insensitive conductance. For the purpose of this study, we have not investigated the molecular identity of this current and shall simply refer to it as I_DHPG. Despite a contribution of I_DHPG to the total inward current evoked by the drug, we can, nonetheless, clearly demonstrate a GBZ-sensitive persistent increase in holding current. In neurons where GBZ was perfused before DHPG application, I_GABAtonic was 34.4 ± 5.0 pA ($n = 6$) (Fig. 1D,F). In contrast, in those neurons in which GBZ was added after DHPG perfusion, I_GABAtonic (which represents the sum of the DHPG-induced increase in I_GABAtonic and basal I_GABAtonic) was 98.2 ± 13.6 pA (a 2.9-fold increase, $n = 6$, $p < 0.01$) (Fig. 1D,F) revealing an apparent increase in I_GABAtonic of 63.8 ± 10.2 pA. This difference was similar ( $p > 0.05$) to that observed in DHPG-induced currents observed in the presence and absence of GBZ (see above), demonstrating that the fraction of DHPG-induced current not produced by I_DHPG is due entirely to increased I_GABAtonic.

In addition to excluding I_DHPG, we were also able to exclude temporal summation of IPSCs as a significant contributing factor to the persistent DHPG-induced inward current by performing recordings in the lateral subdivision of the vLGN-l. Unlike their dorsal counterparts, vLGN neurons do not express δ-subunit containing eGABA_ARs, although kinetic properties of phasic synaptic IPSCs are very similar (Bright et al., 2007). Moreover, it has been demonstrated in the vLGN-l that group I mGluR activation enhances the frequency of GABA_AR-mediated IPSCs in a TTX-insensitive manner (Govindaiah and Cox, 2009). In our experiments in vLGN-l neurons, application of DHPG (100 $\mu$M) increased IPSC frequency (control: 5.8 ± 1.7 Hz; DHPG: 58.8 ± 20.8 Hz, $n = 4$, $p < 0.05$, unpaired $t$ test) (Fig. 2A–C), and occurrence of IPSC bursts (Fig. 2B) similar to the dLGN cells but did not evoke any persistent inward current (Fig. 2A). Thus, IPSC decay kinetics that are similar between dLGN and vLGN appear to be sufficiently rapid to prevent temporal summation of currents even at
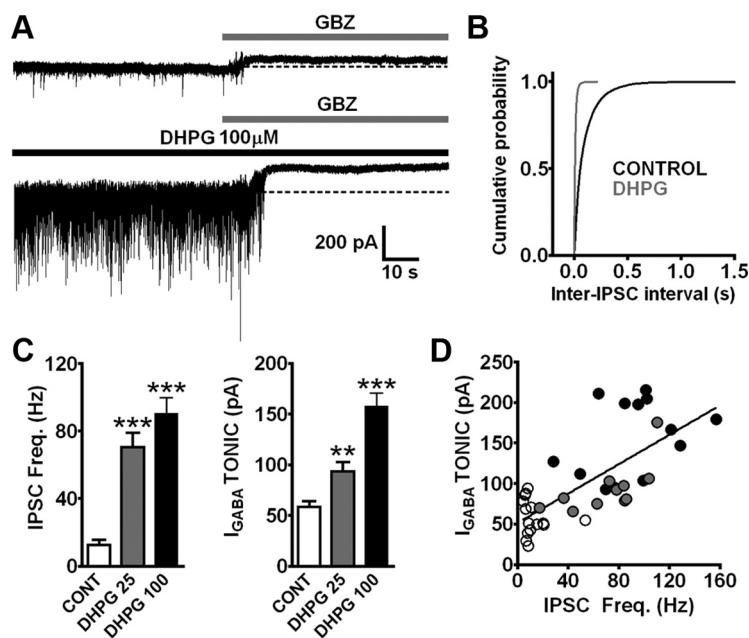


**Figure 3.** Gabazine-sensitive tonic currents are significantly larger in TC neurons in the presence of DHPG. **A**, Representative traces illustrating the significantly larger I_GABAtonic amplitude and increased IPSC frequency in a group of neurons continuously bathed in DHPG (100 $\mu$M) compared with a separate group of control neurons. **B**, Cumulative probability plot of inter-IPSC intervals for all cells under control conditions (black line, $n = 7460$ events from 14 cells) and in the presence of 100 $\mu$M DHPG (gray line, $n = 9370$ events from 12 cells). Note that DHPG causes a leftward shift in distribution compared with control. **C**, Summary of the significant concentration-dependent increases in both IPSC frequency and I_GABAtonic amplitude produced by DHPG (control, $n = 15$; DHPG 25 $\mu$M, $n = 11$; DHPG 100 $\mu$M, $n = 13$). **D**, Plot of I_GABAtonic amplitude versus IPSC frequency shows a significant correlation between the two measurements. Open, gray, and black circles represent control, DHPG 25 $\mu$M, and DHPG 100 $\mu$M data, respectively; and the solid line represents a linear regression fit to all points. **$p < 0.01$, ***$p < 0.001$.

relatively high frequencies. This was further tested by using a simple model of linear IPSC summation based upon the amplitude and weighted $\tau_w$ of IPSCs measured in the dLGN under our control conditions. The mean steady-state current during the model train was calculated as the product of the integral of individual IPSCs (A $\tau_w$) and the inverse of the inter-IPSC interval. Across a range of simulated IPSC frequencies (10–120 Hz), the mean current was insufficient to account for the increased GBZ-sensitive current observed in the presence of DHPG (100 $\mu$M) (Fig. 2D). In support of our experimental findings, these data show that IPSC summation does not make a large contribution to the measured persistent current at similar IPSC frequencies as those evoked by DHPG application.

Due to the presence of I_DHPG, in subsequent experiments, we measured the effects of drugs on GBZ-sensitive I_GABAtonic in different populations of TC neurons and compared them to a separate population of control TC neurons, thereby excluding any contamination of baseline current shifts by non-GABA_AR-mediated mechanisms (unless otherwise indicated). In a control group of dLGN neurons ($n = 15$), IPSC amplitude and $\tau_w$ were similar to those neurons under control conditions before bath application of DHPG, and basal frequency was 9.7 ± 1.4 Hz (Table 1). Focal application of GBZ to these neurons not only blocked all spontaneous IPSCs, but also revealed a I_GABAtonic of 58.9 ± 6.2 pA (Fig. 3A,C). In the continuous presence of 100 $\mu$M DHPG ($n = 13$), IPSC frequency (90.5 ± 9.9 Hz) (Fig. 3A,C), inter-IPSC interval distribution (Fig. 3B), and I_GABAtonic amplitude (158.1 ± 13.5 pA) (Fig. 3A,C), were significantly different compared with control (all $p < 0.001$). I_GABAtonic in the presence of DHPG in these neurons was 2.7-fold larger than control neurons, a value similar to that observed in "wash-in" experiments

(Fig. 1*D*). Moreover, I$_{GABA}$tonic amplitude was also larger compared with control when normalized to whole-cell capacitance (control: 0.9 ± 0.1 pA/pF; DHPG: 2.6 ± 0.2 pA/pF, $p < 0.001$). Because of the large increase in IPSC frequency and the regular presence of IPSC bursts in DHPG, we were unable to retrieve sufficient numbers of isolated IPSCs to make meaningful analysis of either IPSC amplitude or $\tau_w$. Nonetheless, large IPSC bursts were readily apparent in the presence of DHPG, and had a mean interval of 248.0 ± 11.1 ms, similar to that seen following transient bath application of the agonist. Moreover, the effect of DHPG was concentration dependent. In the presence of 25 $\mu$M DHPG ($n = 11$), we observed increases in both I$_{GABA}$tonic amplitude (93.7 ± 9.1 pA, $p < 0.01$) (Fig. 3*C*) and IPSC frequency (70.7 ± 8.6 Hz, $p < 0.001$) that were significantly different from control values but smaller than those observed with 100 $\mu$M. The mean inter-IPSC burst interval was greater in 25 $\mu$M DHPG (279.9 ± 7.7 ms) compared with 100 $\mu$M DHPG. It is therefore clear that the GBZ-sensitive I$_{GABA}$tonic is significantly greater in TC neurons exposed to DHPG compared with those under control conditions.

We next determined whether there was a correlation between vesicular GABA release and tonic current amplitude. Similar to a previous finding (Bright and Brickley, 2008), we observed no correlation between IPSC frequency and I$_{GABA}$tonic amplitude under control conditions ($r = -0.30$, Pearson's test). Likewise, there was no correlation between IPSC frequency and I$_{GABA}$tonic amplitude in the presence of single concentrations of DHPG ($r = 0.34$). However, when control and DHPG data were pooled ($n = 39$) a strong correlation between IPSC frequency and I$_{GABA}$tonic amplitude was found ($r = 0.72$) (Fig. 3*D*). Thus, our data suggest that a causal relationship may exist between vesicular GABA release and I$_{GABA}$tonic, but seemingly only when "global" changes in GABA release occur (Bright and Brickley, 2008).

Subsequently, we tested whether the increased I$_{GABA}$tonic relied upon the presence of the δ-subunit containing eGABA$_A$Rs, which are the predominant eGABA$_A$Rs expressed in the thalamus (Jia et al., 2005, Sur et al., 1999), using δ-subunit knock-out mice ($\delta^{-/-}$). In slices from both WT and $\delta^{-/-}$ mice, bath application of DHPG (100 $\mu$M) produced a large increase in IPSC frequency (535%, $p < 0.001$, $n = 7$; and 433%, $p < 0.01$, $n = 7$, respectively) and a persistent inward current increase (Fig. 4*A*). In WT mice, however, the DHPG-induced current was significantly larger than in $\delta^{-/-}$ mice (WT: 67.3 ± 13.3 pA; KO: 27.6 ± 6.8 pA; $p < 0.05$), indicating a major contribution of δ-subunit-dependent tonic GABAergic activity (Fig. 4*C*). This significantly increased inward current in WT vs $\delta^{-/-}$ mice further excludes the possibility that non-GABAergic mechanisms underpin the mGluR-mediated effect we have observed. When GBZ was applied, a I$_{GABA}$tonic (75.9 ± 8.9 pA) was observed that was significantly greater than in $\delta^{-/-}$ animals (12.2 ± 6.5 pA, $p < 0.001$) (Fig. 4*B*,*C*). Interestingly, in $\delta^{-/-}$ animals, in the presence of DHPG, a residual I$_{GABA}$tonic was observed, suggesting a minor contribution from non-δ-subunit-containing eGABA$_A$Rs as has been previously described in the absence of DHPG (Cope et al., 2009). Thus, activation of group I mGluRs not only increases phasic GABA$_A$ inhibition but also enhances tonic inhibition in TC neurons of the dLGN via increased activation of δ-subunit-containing eGABA$_A$Rs.

### Combined mGluR1a and mGluR5 activation mediates increased tonic inhibition

Although previous work (Govindaiah and Cox, 2006) has reported that increased GABA release from dLGN interneurons is solely mediated by mGluR5, we decided to test whether the
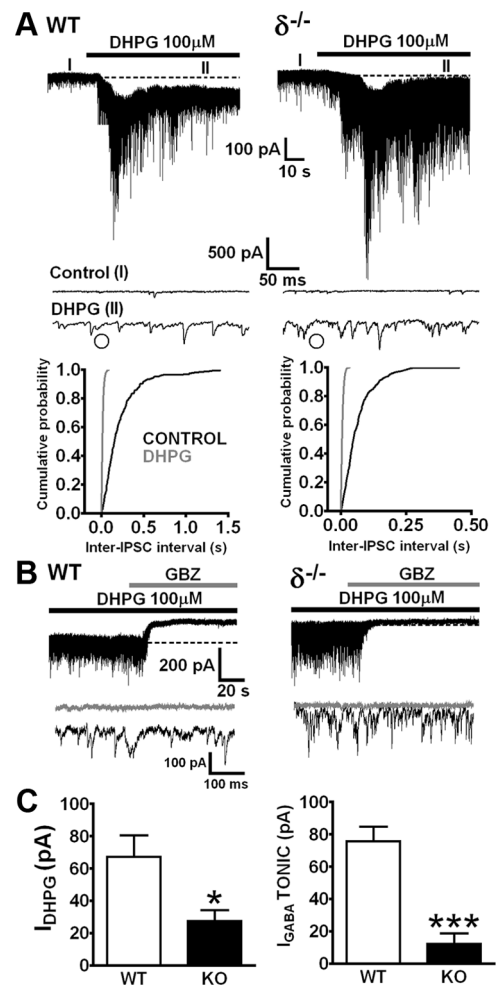


**Figure 4.** Group I mGluR-mediated increase in I$_{GABA}$tonic is dependent upon δ-subunit-containing eGABA$_A$Rs. *A*, dLGN neurons from WT mice show a significant increase in IPSC frequency and a persistent inward shift in holding current upon DHPG (100 $\mu$M) application. Neurons from $\delta^{-/-}$ mice also show significant increases in IPSC frequency but a significantly smaller persistent inward current. Expanded traces show control (*AI*) and DHPG-mediated (*AII*) IPSCs in WT and $\delta^{-/-}$ animals. Note the bursts of IPSCs that are similar to those previously described in rat dLGN neurons (open circles). Cumulative probability distributions for the two neurons illustrated (WT control, $n = 272$ events; WT DHPG, $n = 1374$ events; $\delta^{-/-}$ control, $n = 607$ events; $\delta^{-/-}$ DHPG, $n = 1434$ events) show significant ($p < 0.001$) DHPG-induced left shifts in inter-IPSC interval. *B*, Traces showing I$_{GABA}$tonic revealed by GBZ application (gray bar) in WT and KO mice for two different neurons than those depicted in *A*. Expanded traces illustrate the high IPSC frequency in the presence of DHPG (black) and their complete block by GBZ (gray). Notice the significant shift in the holding current in WT neurons but not in $\delta^{-/-}$ mice. *C*, Comparison of the significantly larger DHPG-induced inward currents in WT versus $\delta^{-/-}$ mouse dLGN neurons. *$p < 0.05$, ***$p$, 0.001.

DHPG-induced increase in I$_{GABA}$tonic was mGluR1a specific or mGluR5 specific. Application of 100 $\mu$M DHPG together with the mGluR1a selective antagonist LY367385 (100 $\mu$M, $n = 14$) reduced I$_{GABA}$tonic amplitude relative to DHPG alone (114.9 ± 7.4 pA, $p < 0.01$) (Fig. 5*C*), but did not significantly affect the DHPG-induced increase in spontaneous IPSC frequency (73.0 ± 6.7 Hz) (Fig. 5*C*) or IPSC burst interval (238.1 ± 7.0 ms). By comparison, application of 100 $\mu$M DHPG together with the mGluR5 selective antagonist MTEP (100 $\mu$M, $n = 8$) reduced both IPSC frequency and I$_{GABA}$tonic amplitude (53.1 ± 4.7 Hz and 101.1 ± 8.6 pA, both $p < 0.01$) (Fig. 5*C*), and increased the IPSC burst interval (317.2 ± 9.0 ms, $p < 0.001$) relative to DHPG alone. Similarly, coapplication of 100 $\mu$M LY367385 and 100 $\mu$M

MTEP with 100 $\mu$M DHPG ($n = 8$) also reduced I$_{GABA}$tonic amplitude and IPSC frequency (97.7 $\pm$ 6.4 pA and 55.9 $\pm$ 8.2 Hz; $p < 0.01$ and 0.05, respectively) (Fig. 5$C$), and increased the IPSC burst interval (339.9 $\pm$ 18.0 ms, $p < 0.001$), compared with DHPG alone. Plotting I$_{GABA}$tonic against IPSC frequency for all tested conditions revealed a significant correlation between both parameters ($r = 0.65$, $p < 0.0001$) (Fig. 5$C$). However, neither individual nor combined block of mGluR1a or mGluR5 was capable of fully reversing the DHPG-induced increases in IPSC frequency and I$_{GABA}$tonic amplitude (all $p < 0.001$ compared with control). Thus, maximal concentrations of selective mGluR1a and mGluR5 antagonists are unable to block the effects of 100 $\mu$M DHPG.

To address this problem, we repeated experiments using the lower concentration of DHPG. In the presence of 25 $\mu$M DHPG, application of 100 $\mu$M LY367385 ($n = 9$) significantly decreased IPSC frequency (31.6 $\pm$ 9.0 Hz, $p < 0.01$), increased IPSC burst interval (436.8 $\pm$ 50.7 ms, $p < 0.01$), but did not significantly reduce I$_{GABA}$tonic amplitude (75.6 $\pm$ 5.9 pA) relative to 25 $\mu$M DHPG alone ($n = 11$) (Fig. 5$C$), although a downward trend in the latter was observed. Similarly, application of 100 $\mu$M MTEP ($n = 13$) together with 25 $\mu$M DHPG significantly decreased IPSC frequency (49.5 $\pm$ 6.0 Hz, $p < 0.05$) and increased IPSC burst interval (462.9 $\pm$ 43.3 ms, $p < 0.001$), but did not significantly reduce tonic current amplitude (78.7 $\pm$ 5.0 pA) (Fig. 5$C$). Under both these conditions, IPSC frequency and I$_{GABA}$tonic amplitude were still larger compared with control ($p < 0.05$). However, coapplication of LY367385 and MTEP together with 25 $\mu$M DHPG ($n = 9$) significantly decreased both IPSC frequency and I$_{GABA}$tonic amplitude compared with 25 $\mu$M DHPG alone (12.5 $\pm$ 3.4 Hz and 57.7 $\pm$ 7.4 pA; $p < 0.001$ and 0.01, respectively) (Fig. 5$A$–$C$), so that values were not significantly different to control ($p > 0.05$). Moreover, coapplication of LY367385 and MTEP increased IPSC burst interval to 879.4 $\pm$ 90.6 ms ($p < 0.001$), although shorter bursts of reduced amplitude were still apparent (Fig. 5$B$). As for 100 $\mu$M DHPG, a significant correlation ($r = 0.64$, $p < 0.0001$) between I$_{GABA}$tonic and IPSC frequency was observed under these conditions (Fig. 5$C$). Thus, in contrast to previous studies we found that the combined activation of both mGluR1a and mGluR5 mediates the DHPG-induced increase in IPSC frequency and eGABA$_A$R-dependent I$_{GABA}$-tonic amplitude.
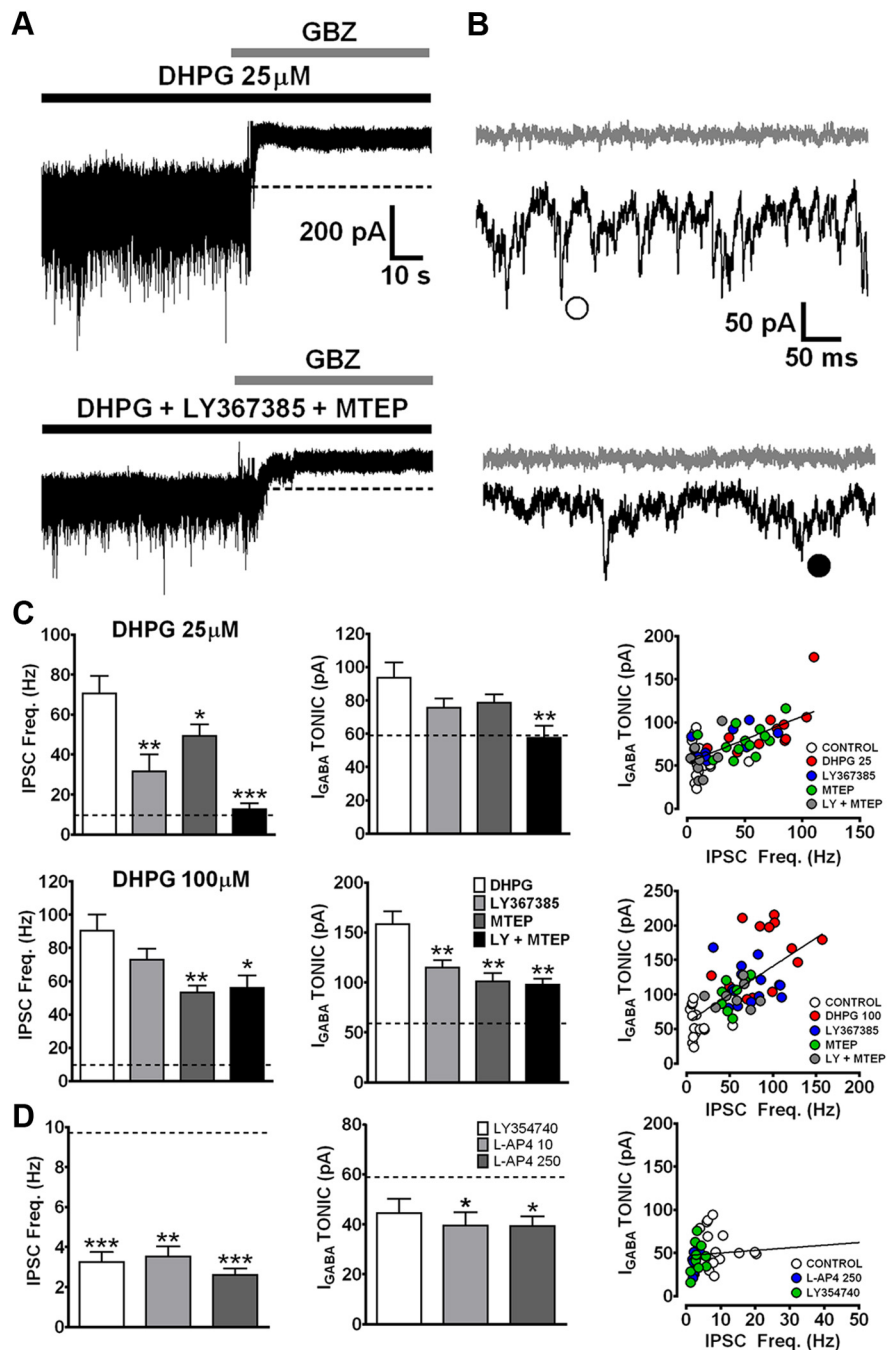


**Figure 5.** Tonic currents are enhanced by activation of mGluRs 1a and 5, and reduced by group II/III mGluR activation. **A**, Representative current traces from different TC neurons of the dLGN in the presence of 25 $\mu$M DHPG alone (black bar, top), and in the combined presence of 25 $\mu$M DHPG, the mGluR1a antagonist LY367385 (100 $\mu$M), and mGluR5 antagonist MTEP (100 $\mu$M) (bottom). I$_{GABA}$tonics were revealed by focal application of GBZ (gray bars). **B**, Expanded current traces from the same cells as in **A** showing that coapplication of DHPG with LY367385 and MTEP decreases the frequency of IPSCs. Note that large IPSC bursts (open circle) are prevalent in the presence of DHPG alone, but bursts of reduced amplitude and duration occur even in the combined presence of DHPG, LY367385, and MTEP (filled circle). **C**, Summary of the effects of LY367385 and MTEP in isolation and in combination upon DHPG-induced increases in IPSC frequency and I$_{GABA}$tonic. Combined application of both antagonists completely blocked the effects of 25 $\mu$M DHPG. Control levels are indicated by dashed lines. Plot of I$_{GABA}$tonic against IPSC frequency for individual neurons under all tested conditions (both 25 and 100 $\mu$M DHPG) shows the significant correlation between both parameters. Note the block of DHPG (25 $\mu$M, red) effect in all cells by combined application of LY367385 and MTEP (gray). Black lines represent linear regression fits to the pooled data. **D**, Groups II and III mGluRs modulate GABA release. Graphs show the effects of the group II mGluR agonist LY354740 (10 $\mu$M) and group III agonist L-AP4 (10 and 250 $\mu$M) on IPSC frequency and I$_{GABA}$tonic amplitude. There is no significant correlation between I$_{GABA}$tonic and IPSC frequency under these conditions ($p > 0.05$). *$p < 0.05$, **$p < 0.01$, ***$p < 0.001$.
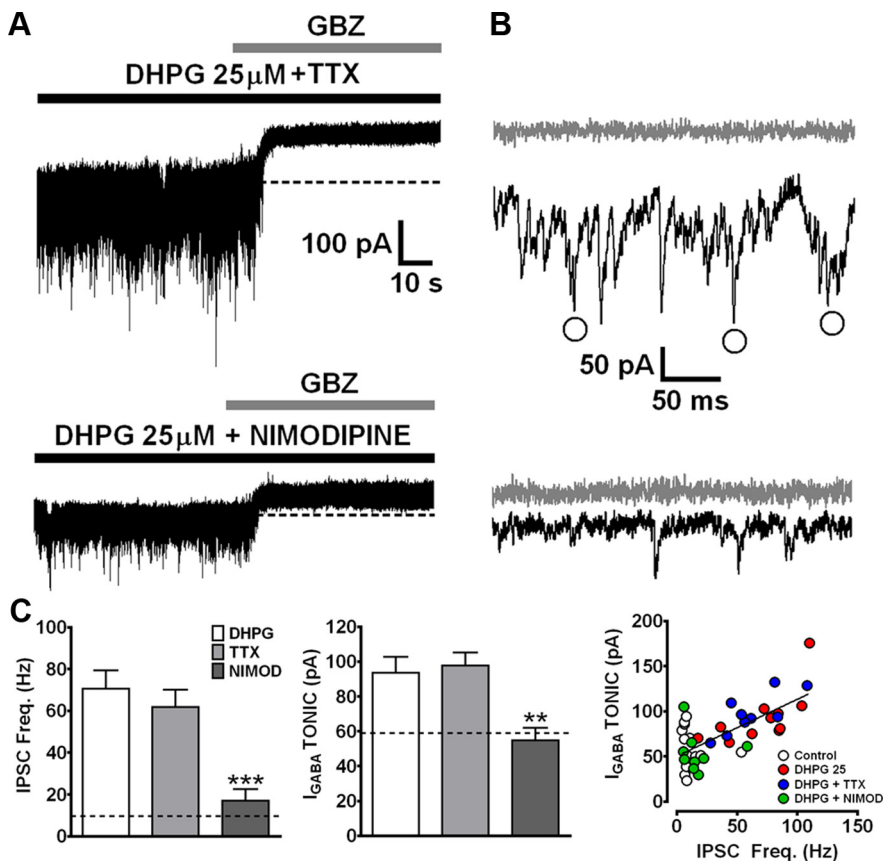
**Figure 6.** Effects of DHPG are L-type Ca$^{2+}$ channel-dependent but TTX insensitive. **A**, Representative current traces from different TC neurons of the dLGN in the presence of 25 $\mu$M DHPG and 0.5 $\mu$M TTX (black bar, top) and in the presence of 25 $\mu$M DHPG and 10 $\mu$M nimodipine (black bar, bottom). I$_{GABA}$tonics were revealed by focal application of GBZ (gray bars). **B**, Expanded current traces from the same cells as in **A** showing that application of nimodipine, but not TTX, blocks the DHPG-induced increase in sIPSC frequency and I$_{GABA}$tonic. Note the prevalence of IPSC bursts (open circles) in the presence of DHPG and TTX, but their absence in the presence of DHPG and nimodipine. **C**, Comparison of the effects of TTX and nimodipine on DHPG-induced increases in IPSC frequency and I$_{GABA}$tonic amplitude. Dotted lines represent the mean values of IPSC frequency and I$_{GABA}$tonic amplitude under control conditions. **$p < 0.01$, ***$p < 0.001$ vs DHPG alone.

### Group II and group III mGluRs modulate tonic inhibition

Activation of group II and group III mGluRs has been shown to reduce phasic inhibition in TC neurons (Govindaiah and Cox, 2006); therefore, we examined whether their activation also affected tonic inhibition. Application of the group II (i.e., mGluRs 2 and 3) selective agonist LY354740 (10 $\mu$M, $n = 10$) reduced IPSC frequency compared with control ($3.3 \pm 0.5$ Hz, $p < 0.001$), but did not significantly reduce I$_{GABA}$tonic amplitude ($44.5 \pm 5.9$ pA), although there was a clear trend for smaller tonic currents (Fig. 5D). By comparison, application of the group III agonist L-AP4, at a concentration selective for mGluRs 4 and 8 (10 $\mu$M, $n = 10$), not only significantly reduced IPSC frequency ($3.5 \pm 0.5$ Hz, $p < 0.01$), but also reduced I$_{GABA}$tonic amplitude ($39.4 \pm 5.7$ pA, $p < 0.05$) (Fig. 5D). Increasing the concentration of L-AP4 to 250 $\mu$M ($n = 9$) caused no further decrease in either IPSC frequency ($2.6 \pm 0.3$ Hz) or I$_{GABA}$tonic amplitude ($39.3 \pm 3.6$ pA), indicating no contribution of mGluR7 to this effect (Fig. 4D). Unlike the effect of DHPG, when I$_{GABA}$tonic was plotted against IPSC frequency in the presence of group II/III mGluR agonists no significant correlation was observed between both measurements ($r = 0.26$, $p = 0.46$) (Fig. 5D). Thus, activation of mGluRs 4 and 8 can modulate vesicular GABA release and control tonic inhibition. Furthermore, despite the lack of a significant reduction in I$_{GABA}$tonic amplitude in the presence of LY354740, the signifi-

cant reduction in IPSC frequency and a clear downward trend in I$_{GABA}$tonic amplitude also indicate a likely contribution of mGluRs 2 and/or 3.

### Increased tonic inhibition is L-type Ca$^{2+}$ channel dependent

Thalamic interneurons can release GABA through action potential-dependent and action potential-independent mechanisms, apparently corresponding to release from axonal F1 and dendritic F2 terminals, respectively (Cox and Sherman, 2000; Govindaiah and Cox, 2006). We therefore tested whether the mGluR1a- or mGluR5-mediated increases in tonic inhibition were action potential dependent by testing whether TTX (0.5 $\mu$M), coapplied with either LY367385 or MTEP, could block the effects of 25 $\mu$M DHPG. Application of TTX together with DHPG and LY367385 ($n = 10$), to test the action potential dependence of mGluR5-mediated effects, caused no further reduction in either I$_{GABA}$tonic amplitude or IPSC frequency compared with the application of just DHPG and LY367385 together ($74.8 \pm 5.9$ pA and $32.6 \pm 8.1$ Hz, respectively). Similarly, applying TTX together with DHPG and MTEP ($n = 8$), to test the action potential dependence of mGluR1a-mediated effects, had no further effect on either I$_{GABA}$tonic amplitude or IPSC frequency compared with the application of just DHPG and MTEP together ($88.4 \pm 11.3$ pA and $41.4 \pm 9.6$ Hz). Thus, neither mGluR1a- or mGluR5-mediated increases in tonic inhibition are action potential dependent. To test for any action potential dependence of DHPG effects in general, we applied only TTX with 25 $\mu$M DHPG ($n = 9$). Coapplication had no effect on I$_{GABA}$tonic amplitude or IPSC frequency compared with DHPG alone ($97.8 \pm 8.0$ pA and $61.9 \pm 8.8$ Hz) (Fig. 6A,C), and IPSC bursts were readily apparent in the presence of TTX with the burst interval significantly shorter compared with 25 $\mu$M DHPG alone ($245.5 \pm 12.3$ ms, $p < 0.01$) (Fig. 6A). F1 terminals, therefore, appear to have a negligible contribution to mGluR-mediated increases in either phasic or tonic GABA$_A$ inhibition, contrary to previous findings (Cox and Sherman, 2000).

However, a recent study (Acuna-Goycolea et al., 2008) indicated that L-type Ca$^{2+}$ channels appear to be critically involved in GABA release from F2, but not F1, terminals. Therefore, we tested whether the mGluR-mediated increase in I$_{GABA}$tonic is also L-type Ca$^{2+}$ channel dependent. Application of the L-type Ca$^{2+}$ channel blocker nimodipine (10 $\mu$M) together with 25 $\mu$M DHPG ($n = 9$) caused a significant reduction in both I$_{GABA}$tonic amplitude and IPSC frequency compared with 25 $\mu$M DHPG alone ($54.7 \pm 7.8$ pA and $17.1 \pm 5.8$ Hz; $p < 0.01$ and 0.001, respectively) (Fig. 6A,C), and significantly increased the IPSC burst interval ($1090.6 \pm 17.7$ ms, $p < 0.001$) (Fig. 6B). In fact, values of I$_{GABA}$tonic amplitude and IPSC frequency were not significantly different to those seen under control conditions (both $p > 0.05$). There was a significant correlation ($r = 0.69$, $p < 0.0001$) between I$_{GABA}$tonic and IPSC frequency when the data

were plotted for these conditions (Fig. 6C). Furthermore, we tested the effects of TTX and nimodipine on the changes in phasic and I$_{GABA}$tonic following application of 100 μM DHPG. Coapplication of TTX with 100 μM DHPG ($n = 11$) did not significantly affect IPSC frequency (85.1 ± 9.1 Hz), IPSC burst interval (233.4 ± 10.4 ms), or I$_{GABA}$tonic amplitude (149.9 ± 10.6 pA) compared with 100 μM DHPG alone. However, coapplication of nimodipine and 100 μM DHPG ($n = 8$) significantly decreased both IPSC frequency (26.3 ± 3.5 Hz, $p < 0.001$) and I$_{GABA}$tonic amplitude (55,4 ± 9.2 pA, $p < 0.001$), although only I$_{GABA}$tonic amplitude returned to control levels, and increased the IPSC burst interval (1042.7 ± 72.0 ms, $p < 0.001$) compared with DHPG alone. In summary, these data show that mGluR-induced GABA release is action potential independent but L-type Ca$^{2+}$ channel dependent, suggesting that mGluRs 1a and 5 control GABA release almost exclusively from F2 terminals.

### Activation of group I mGluRs does not increase tonic inhibition in TC neurons of the VB thalamus

To confirm the apparent requirement of F2 terminals in the mGluR-mediated modulation of tonic current, we performed recordings from VB thalamic neurons. Unlike the dLGN, the rodent VB thalamus contains no interneurons (Barbaresi et al., 1986; Harris and Hendrickson, 1987), and GABAergic innervation is provided solely by neurons of the NRT. We therefore tested whether activation of group I mGluRs also modulates vesicular GABA release and I$_{GABA}$tonic amplitude in TC neurons of the VB. In the control population of VB TC neurons ($n = 10$), IPSC properties (Table 1) and I$_{GABA}$tonic amplitude were similar to those described previously (Fig. 7A) (Belelli et al., 2005; Cope et al., 2005, 2009; Jia et al., 2005). In contrast to TC neurons of the dLGN, however, 100 μM DHPG ($n = 7$) had no significant affect on either IPSC frequency (control: 6.8 ± 0.7 Hz; DHPG: 7.9 ± 1.4 Hz) or I$_{GABA}$tonic amplitude (control: 90.7 ± 7.8 pA; DHPG: 112.5 ± 18.9 pA) (Fig. 7A), although there was a trend for both to be slightly increased. However, whereas there was a trend toward a leftward shift in the distribution of inter-IPSC intervals in the presence of DHPG compared with control ($p < 0.01$) normalized I$_{GABA}$tonic amplitude was no different in the presence and absence of DHPG (control: 1.3 ± 0.1 pA/pF; DHPG: 1.4 ± 0.2 pA/pF).

The lack of effect of DHPG upon phasic and tonic inhibition in the VB thalamus suggested that group I mGluR receptors do not modulate output from neurons of the NRT, the sole GABAergic inputs into these nuclei. To test this, we made current-clamp recordings from NRT neurons, which we identified by their position within the slice, their characteristic electrophysiological properties, and by *post hoc* histochemistry (Fig. 7B). These neurons displayed relatively hyperpolarized resting membrane potentials (−74.9 ± 2.3 mV uncorrected for liquid junction potential, $n = 8$), and although DHPG (100 μM) produced depolarizing responses in all cells tested (18.2 ± 2.9 mV), this was sufficient to evoke action potential firing in only 50% of neurons tested. On average, the firing frequency in response to DHPG of the NRT neurons examined was only 4.2 ± 2.6 Hz (maximum 20.4 Hz). Thus, under our conditions *in vitro*, DHPG does not control tonic inhibition in VB thalamic TC neurons because it cannot modulate GABA release from the NRT. In addition, our findings suggest that an NRT-mediated contribution to increased I$_{GABA}$tonic in the dLGN is negligible. This does not however, discount a potential mGluR-dependent modulatory role for NRT neurons *in vivo* where they are often resting at much more depo-
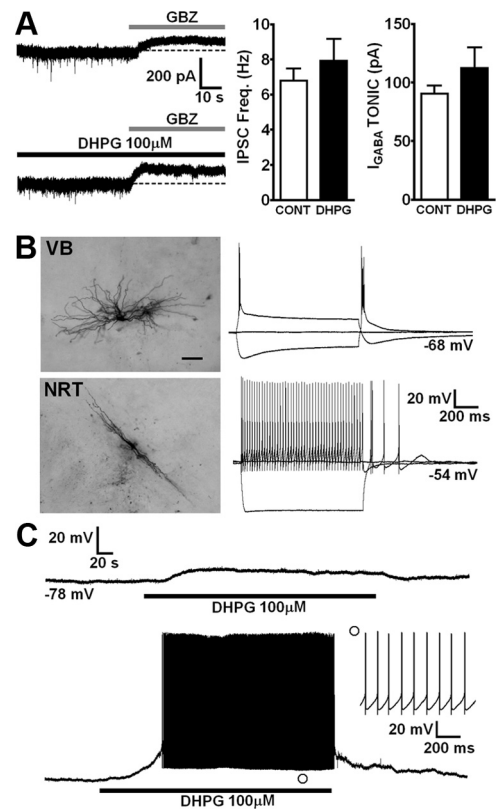


**Figure 7.** DHPG does not affect phasic and tonic inhibition in TC neurons of the VB. **A**, Representative current traces from different TC neurons of the VB thalamus under control conditions (top) and in the continuing presence of DHPG (100 μM, bottom). Focal application of GBZ (100 μM, gray bar) reveals I$_{GABA}$tonic of similar magnitude in both neurons. Summary of the effects of DHPG on IPSC frequency and I$_{GABA}$tonic (control: $n = 10$; DHPG: $n = 7, p > 0.05$). **B**, Typical examples of current-clamp recordings made from neurons in the VB and NRT. Cells were filled through the patch pipette with biocytin to reveal characteristic and distinct dendritic morphologies. **C**, DHPG (100 μM) depolarized the membrane potential sufficiently to evoke action potentials in only 4 of 8 NRT neurons tested.

larized potentials as a result of sustained neuromodulatory influences that are absent *in vitro*.

### Synaptic activation of mGluRs enhances tonic currents in the dLGN

Finally, we sought to determine whether synaptic activation of interneuronal mGluRs was able to modulate I$_{GABA}$tonic in the dLGN. To do this, we used a slice preparation designed to maximize connectivity of RGC axons in the optic tract with the dLGN. This allowed us to exploit the specialized "triadic" synaptic circuitry of RGC, TC neuron, and interneuron connections in the dLGN (Fig. 8A,B). Under control conditions, electrical stimulation of the optic tract several millimeters away from the recording site resulted in a range of responses. Low-intensity single stimuli (70 μA) typically produced monosynaptic EPSCs in TC neurons that were characteristically depressing at short interstimulus intervals (30 ms) (Fig. 8C). Increasing stimulus intensity (>~100 μA) typically resulted in recruitment of disynaptic inhibition, which was in the form of both fast and/or delayed GABAergic IPSCs (Fig. 8C middle), as has been previously described (Acuna-Goycolea et al., 2008). Delayed IPSCs occurred with a latency of several tens of milliseconds after the single stimulus. In all neurons tested ($n = 12$), application of the ionotropic glutamate receptor [iGluR (AMPA/NMDA)] antagonists CNQX (50 μM) and D-AP5 (50 μM) completely blocked both monosynaptic ex-
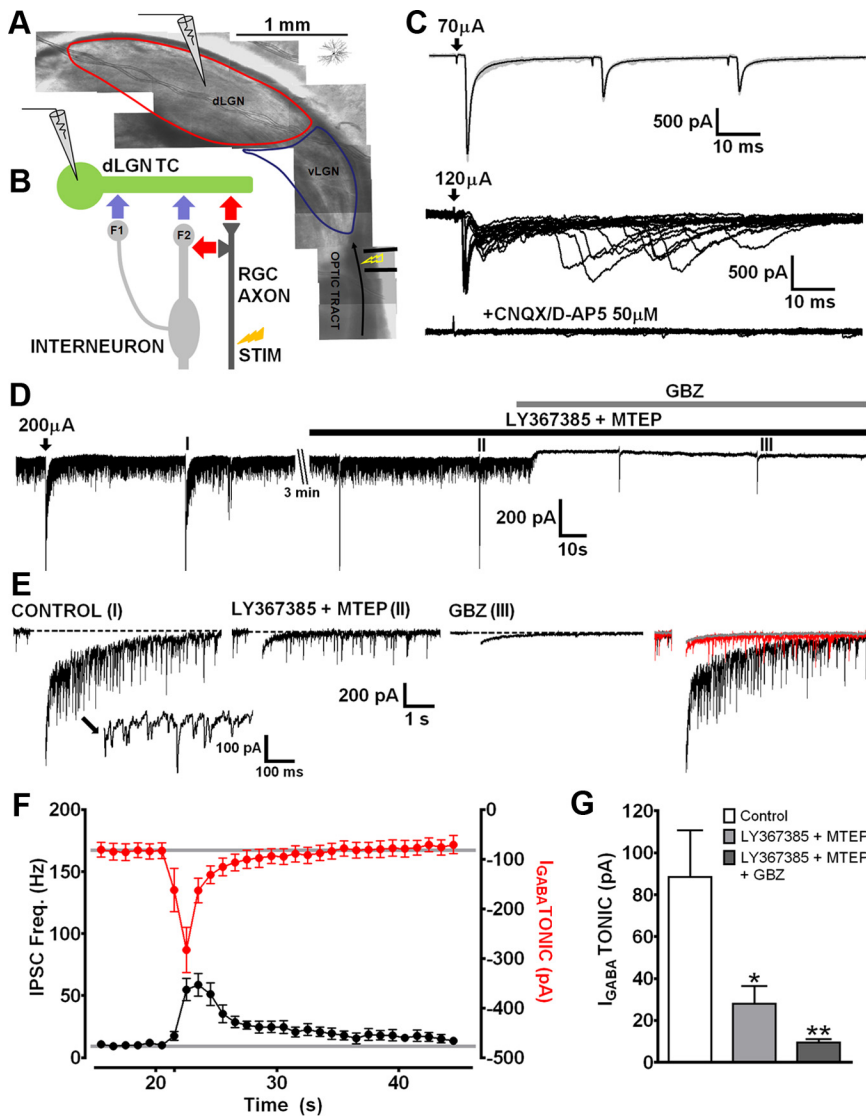
**Figure 8.** Synaptic activation of interneuron mGluRs modulates I$_{GABA}$tonic in TC neurons of the dLGN. **A**, Photomicrograph of the angled slice preparation used to preserve connectivity of inputs from retinal ganglion cell axons into dLGN. Recording and stimulating locations are illustrated. **B**, A schematic representation of the triadic circuitry of RGC axon, interneuron, and TC connectivity in dLGN. Excitatory synapses are represented by red arrows, and inhibitory synapses by blue arrows. **C**, Weak stimulation of the optic tract mostly recruited monosynaptic EPSCs, which were strongly depressing at short interstimulus intervals typical of RGC inputs to dLGN neurons. In a different neuron, stronger stimulation produced monosynaptic EPSCs and disynaptic IPSCs. Fast and delayed IPSCs were commonly observed, suggesting release from both F1 and F2 dendrodendritic terminals as previously described (Acuna-Goycolea et al., 2008). Inhibition of AMPA/NMDA glutamate receptors by CNQX and D-AP5 (50 μM each) blocked evoked EPSCs and both fast and delayed IPSCs. **D**, Tetanic stimulation of the optic tract resulted in a marked and sustained increase in IPSC frequency and an increase in the holding current. LY367385 and MTEP (100 μM) were applied for 3 min and produced significant inhibition of the tetanus-evoked response. Bath application of GBZ revealed I$_{GABA}$tonic. **E**, Expanded traces (stimulus artifact removed for clarity) show the stimulus evoked responses under control (**EI**), LY367385 and MTEP (**EII**), and LY367385, MTEP, and GBZ (**EIII**), respectively. Inset in **EI** shows tetanically evoked bursts of IPSCs similar to those observed with bath application of DHPG. The traces are shown overlaid on the right. **F**, Time course of tetanically evoked I$_{GABA}$tonic and IPSC frequency increase for cells under control conditions (n = 7). I$_{GABA}$tonic is calculated by subtraction of evoked responses in GBZ (**EIII**) from control responses (**EI**) and are binned in 1 s intervals. **G**, Comparison of the stimulus-evoked change in raw mean holding current for 5 s periods after the stimulus under each condition (n = 5 different neurons from those shown in F). *p < 0.05, **p < 0.01.

iGluR blockers we selectively activated interneuron mGluRs by tetanic stimulation (40 pulses, 200 Hz) of the optic tract fibers (Fig. 8D,E). This resulted in a significant increase in IPSC frequency (maximum: 59.1 ± 9.8 Hz; prestimulus: 10.61 ± 1.9 Hz; p < 0.001, n = 7), which was sustained for several seconds after the stimulus (Fig. 8E,F) and was accompanied by a concurrent increase in holding current. Stimulation was repeated twice at 60 s intervals before and after bath application of GBZ. By subtraction of evoked responses in the presence of bath-applied GBZ from control data, a synaptically evoked increase in I$_{GABA}$tonic was revealed. Stimulus-evoked I$_{GABA}$tonic had a peak amplitude of −282.4 ± 45.2 pA (n = 7), which was significantly (p < 0.01) different from the mean I$_{GABA}$tonic in the 5 s before the stimulus (−82.8 ± 15.6 pA) (Fig. 8F). Furthermore, in a separate group of neurons coapplication of LY367385 (100 μM) and MTEP (100 μM) significantly reduced the effects of stimulation on both IPSC frequency and increase in holding current (Fig. 8D,E,G). The amplitude of the stimulation-evoked mean increase in holding current (measured in a 5 s bin after the stimulus) was reduced from 88.4 ± 22.4 pA under control conditions to 27.95 ± 8.5 pA (p < 0.05, n = 5) in the presence of group I mGluR blockers (Fig. 8G). Thus, we show that mGluR-dependent synaptic activation of dLGN interneurons produces enhanced GABA release that not only results in increased disynaptic phasic inhibition in TC neurons but also dynamically regulates eGABA$_A$R-dependent tonic inhibition.

## Discussion

Previous studies have clearly demonstrated that phasic feedforward inhibition in TC neurons of the dLGN is regulated by mGluR-dependent modulation of GABA release from interneurons (Cox et al., 1998; Cox and Sherman, 2000; Govindaiah and Cox, 2004, 2006). Our present results significantly expand these findings by demonstrating that group I mGluR-mediated modulation in the dLGN not only results in increased phasic inhibition but also enhanced tonic GABAergic inhibition in TC neurons. Indeed, we demonstrate for the first time that activation of group I mGluRs by stimulation of optic tract inputs to the dLGN results in dynamic increases in I$_{GABA}$tonic. The failure of previous studies to observe similar mGluR-dependent increases in I$_{GABA}$tonic can be readily explained by two significant factors. First, and most simply, these studies were not specifically looking for enhanced I$_{GABA}$tonic, in fact most were performed before the first description of I$_{GABA}$tonic in the thal-

citatory responses and disynaptic inhibitory fast and delayed responses (Fig. 8C, bottom). Axons from RGCs form synaptic connections onto both TC neuron and interneuron dendrites. Crucially, however, RGC synapses onto TC neurons do not contain mGluRs (which are only found postsynaptically to corticothalamic inputs into these neurons), whereas retinal input does activate mGluRs in dLGN interneurons. Thus, in the presence of

amus (Cox et al., 1998; Cox and Sherman, 2000; Govindaiah and Cox, 2004; Belelli et al., 2005; Cope et al., 2005; Jia et al., 2005). Second, the age of many of the animals used in previous studies (P10–P20 compared with P21–P25 in our study) was often younger than that at which significant expression of eGABA$_A$Rs is observed.

Interestingly, unlike previous findings (Govindaiah and Cox, 2006), our data suggest that mGluR-dependent modulation is mediated by both mGluR1a and mGluR5 on thalamic interneurons and results in sufficient GABA spillover from synaptic terminals to significantly increase I$_{GABA}$tonic. Moreover, it is apparent that there is a clear correlation between the enhanced frequency of GABA release from interneurons and the increased I$_{GABA}$tonic in dLGN TC neurons. In agreement with previous findings in dLGN (Cox and Sherman, 2000; Govindaiah and Cox, 2006), we found little sensitivity of mGluR-mediated effects to TTX, suggesting only a minor contribution of conventional action potential-dependent axonal release from F1 terminals. This finding was complemented by a lack of effect of DHPG in the VB thalamus where interneurons are not present (Barbaresi et al., 1986; Harris and Hendrickson, 1987) and NRT neurons provide the solitary source of GABAergic input via F1 terminals. Although earlier reports indicated a TTX-sensitive increase in IPSC frequency in rodent VB with the nonselective mGluR agonist ACPD (Cox and Sherman, 2000), this could not be replicated in later studies using DHPG (Govindaiah and Cox, 2006), suggesting, in conjunction with our results, that group I mGluRs are absent from NRT terminals. Furthermore, in contrast to previous work we did not find evidence for the presence of distinct populations of neurons in the rat dLGN that were differentially sensitive to TTX, suggesting that most, if not all, TC neurons in the rodent participate in triads with interneurons. Fascinatingly, our data reveal that the mGluR1a- and mGluR5-dependent increases in IPSC frequency and I$_{GABA}$tonic are completely absent in the presence of L-type voltage-gated Ca$^{2+}$ channel blockers. Together, these results strongly suggest that mGluR1a- and mGluR5-dependent enhancement of GABA release from dLGN interneurons is mediated solely by F2-type terminals found at dendrodendritic release sites. Additionally, experiments performed in $\delta^{-/-}$ mice confirm that the extrasynaptic receptors recruited by mGluR-dependent enhancement of GABA spillover from F2 terminals contain GABA$_A$ receptor $\delta$-subunits. Finally, we show that the increase in inward currents we observed was not dependent upon IPSC summation. This is similar to the findings presented by Glykys and Mody (2007) in CA1 pyramidal cells where enhanced I$_{GABA}$tonic in control animals, resulting from sucrose-induced IPSC bursts (at up to 65 Hz), were absent in $\alpha$5- and $\delta$-subunit double-KO mice. Thus, for the first time we functionally demonstrate that eGABA$_A$Rs are located at putative postsynaptic locations on TC neuron dendrites that participate in the triadic circuitry characteristic of the dLGN and that these receptors can be dynamically activated by robust dendrodendritic GABA release (Fig. 9). It is important to note, however, that anatomical data demonstrating the presence of $\delta$-subunit-containing eGABA$_A$Rs in glomeruli remains to be obtained and our
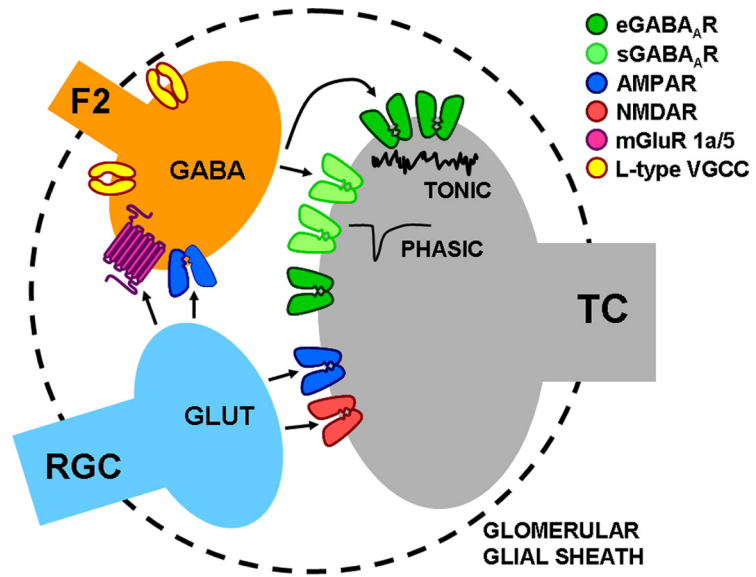


**Figure 9.** Extrasynaptic GABA$_A$Rs are present on TC neuron dendrites postsyanptic to F2 terminals in triads. A schematic illustration depicting the important channels and receptors regulating GABA release and activation of eGABA$_A$Rs in triads. Types 1a and 5 mGluRs are located only on F2 interneuronal terminals and are activated by strong excitatory input from RGCs to induce prolonged L-type voltage-gated Ca$^{2+}$ channel-dependent GABA release. Accumulation and spillover of GABA within the glomerulus is sufficient to increase eGABA$_A$R activation and enhance I$_{GABA}$tonic. This may be assisted by the glial sheath surrounding the glomerulus that prevents juxtaposition of glial processes with these synapses and could impare GABA reuptake by GAT1/GAT3. sGABA$_A$R, Synaptic GABA$_A$ receptor.

findings do not exclude the possibility of eGABA$_A$Rs outside of the glomeruli in dLGN TC neurons.

The presence of eGABA$_A$Rs on dendrites that are postsynaptic to F2 dendritic release sites is particularly fascinating because of the glial ensheathment of the triadic circuitry within the glomerulus (Szentagothai, 1963). Glial cells, in particular astrocytes, are the only cell type within the dLGN that express GABA transporters (GAT-1 and GAT-3) (De Biasi et al., 1998) and as such are entirely responsible for GABA reuptake within the visual thalamus. The absence of glial processes from the ensheathed glomerulus may thus impose a significantly lower spatiotemporal restriction upon GABA diffusion from F2 terminals allowing greater extrasynaptic GABA accumulation and more robust activation of eGABA$_A$Rs compared with extraglomerular F1-type synapses, which are directly juxtaposed to glial processes (Sherman, 2004). This is analogous to a mechanism proposed for tonic current modulation in the glomerular structure surrounding mossy fiber to granule cell synapses in the cerebellum (Wall and Usowicz, 1997; Rossi et al., 2003). It is therefore likely that F2 terminal-mediated GABA release can produce relatively long-lasting changes in tonic GABA$_A$ signaling that may be restricted to a single triad or glomerulus. As such, during intense retinal input sufficient to activate interneuron mGluRs, activation of eGABA$_A$Rs through enhanced GABA release may act to locally inhibit focused dendritic regions and damp down further strengthening input from specific RGCs. In fact, because I$_{GABA}$tonic is estimated to contribute ~80–90% of the total GABA$_A$ receptor-mediated inhibition in TC neurons under basal conditions (dLGN: Cope et al., 2005; VB: Belelli et al., 2005), transiently enhanced I$_{GABA}$tonic within the glomerulus could contribute more strongly to inhibition through shunting mechanisms than increased phasic IPSCs. Intriguingly, this mechanism could represent a potential molecular mechanism for thalamic level adjustment of visual contrast gain by facilitating long-lasting reduction in TC neuron responsiveness to retinal inputs (Sherman, 2004).

Thus, as RGC firing increases monotonically with increased contrast in the external visual stimulus, progressive recruitment of mGluRs 1a and 5 enhances tonic GABAergic inhibition, thereby reducing TC neuron gain. Another potential contribution of relatively long-lasting inhibition by enhanced I$_{GABA}$tonic may be to control dendritic branch-specific spatial regulation of intrinsic dendritic Ca$^{2+}$ signals produced by backpropagating action potentials or low-threshold Ca$^{2+}$ spikes (Errington et al., 2010, Crandall et al., 2010). In this way, I$_{GABA}$tonic may have a significant role in integration of both local and global dendritic signals.

The reliance of mGluR-dependent enhancement of I$_{GABA}$tonic upon L-type Ca$^{2+}$ channels is consistent with GABA release from F2 terminals that is dependent upon dendritic Ca$^{2+}$ spikes in interneurons. Previous anatomical and electrophysiological studies have suggested that group I mGluRs are located on F2 terminals (Godwin et al., 1996, Cox and Sherman, 2000) and that their activation leads to local dendritic signals that are independent of membrane potential changes at the interneuron soma (Govindaiah and Cox, 2004, 2006). An elegant Ca$^{2+}$ imaging study by Acuna-Goycolea et al. (2008) proposed that Ca$^{2+}$ spikes in dLGN interneurons can be readily initiated by synaptic inputs from RGCs, that they produce large intracellular [Ca$^{2+}$] accumulation that can be restricted to dendrites and are dependent upon L-type Ca$^{2+}$ channels. Moreover, they suggest that L-type Ca$^{2+}$ channel-dependent dendritic spikes, which evoke Ca$^{2+}$ signals that last several hundred milliseconds, contribute to delayed disynaptic inhibition by triggering dendritic GABA release. Thus, it appears likely that activation of group I mGluRs on F2 terminals can initiate local L-type Ca$^{2+}$ channel-dependent dendritic Ca$^{2+}$ spikes that results in dendrodendritic GABA release. Furthermore, the slow kinetics of mGluR-dependent EPSCs and dendritic Ca$^{2+}$ spikes can explain the sustained release of GABA after relatively short but intense retinal stimuli. Such long-lasting responses may be necessary to provide sufficient GABA accumulation in the extrasynaptic space of the glomerulus to activate eGABA$_A$Rs, ensuring that enhancement of tonic inhibition occurs only during periods of intense or sustained retinal activity.

Nonetheless, it has also been demonstrated that synaptic activation of dLGN interneurons can induce sustained intrinsic oscillatory multispike bursting at the somatic level (Zhu et al., 1999). This is interesting in light of the pseudo-oscillatory IPSC bursts we observed in TC neurons in the presence of DHPG (Fig. 1C) and after tetanic stimulation (Fig. 7E) of the optic tract, where interburst intervals (200–300 ms) were similar to those described in the aforementioned study. It therefore seems plausible that mGluR activation could provide sufficient depolarization (Govindaiah and Cox, 2006) at the somatic level to induce such rhythmic activity. However, the intrinsic oscillatory bursting observed in thalamic interneurons was highly Na$^+$ channel dependent, whereas the mGluR-evoked increases in IPSC frequency and I$_{GABA}$tonic in our study were insensitive to block by TTX. Thus, our data fit more closely with the former hypothesis and support previous findings that suggest mGluR-dependent enhancement of GABA release occurs independently of action potential discharge.

In conclusion, our results show that expression of δ-subunit-containing eGABA$_A$Rs in the triadic synaptic circuitry within the dLGN and their dynamic modulation by mGluR-dependent interneuron GABA release may play a significant role in visual processing within the thalamus. In fact, along with effects on GABA$_B$ receptors (including presynaptic inhibition of RGC terminals) and increased phasic IPSCs, enhanced eGABA$_A$R-mediated I$_{GABA}$tonic represents the third element of a "triad of inhibition" within the anatomical triads of the dLGN in response to retinal input.

## References

Acuna-Goycolea C, Brenowitz SD, Regehr WG (2008) Active dendritic conductances dynamically regulate GABA release from thalamic interneurons. Neuron 57:420–431.

Barbaresi P, Spreafico R, Frassoni C, Rustioni A (1986) GABAergic neurons are present in the dorsal column nuclei but not in the ventroposterior complex of rats. Brain Res 382:305–326.

Belelli D, Peden DR, Rosahl TW, Wafford KA, Lambert JJ (2005) Extrasynaptic GABA$_A$ receptors of thalamocortical neurons: a molecular target for hypnotics. J Neurosci 25:11513–11520.

Berardi N, Morrone MC (1984) The role of γ-aminobutyric acid mediated inhibition in the response properties of cat lateral geniculate nucleus neurones. J Physiol 357:505–523.

Blitz DM, Regehr WG (2005) Timing and specificity of feed-forward inhibition within the LGN. Neuron 45:917–928.

Bright DP, Brickley SG (2008) Acting locally but sensing globally: impact of GABAergic synaptic plasticity on phasic and tonic inhibition in the thalamus. J Physiol 586:5091–5099.

Bright DP, Aller MI, Brickley SG (2007) Synaptic release generates a tonic GABA$_A$ receptor-mediated conductance that modulates burst precision in thalamic relay neurons. J Neurosci 27:2560–2569.

Cope DW, Hughes SW, Crunelli V (2005) GABA$_A$ receptor-mediated tonic inhibition in thalamic neurons. J Neurosci 25:11553–11563.

Cope DW, Di Giovanni G, Fyson SJ, Orbán G, Errington AC, Lorincz ML, Gould TM, Carter DA, Crunelli V (2009) Enhanced tonic GABA$_A$ inhibition in typical absence epilepsy. Nat Med 15:1392–1398.

Cox CL, Sherman SM (2000) Control of dendritic outputs of inhibitory interneurons in the lateral geniculate nucleus. Neuron 27:597–610.

Cox CL, Zhou Q, Sherman SM (1998) Glutamate locally activates dendritic outputs of thalamic interneurons. Nature 394:478–482.

Crandall SR, Govindaiah G, Cox CL (2010) Low-threshold Ca$^{2+}$ current amplifies distal dendritic signalling in thalamic reticular neurons. J Neurosci 30:15419–15429.

Crunelli V, Haby M, Jassik-Gerschenfeld D, Leresche N, Pirchio M (1988) Cl$^-$- and K$^+$-dependent inhibitory postsynaptic potentials evoked by interneurones of the rat lateral geniculate nucleus. J Physiol 399:153–176.

De Biasi S, Vitellaro-Zuccarello L, Brecha NC (1998) Immunoreactivity for the GABA transporter-1 and GABA transporter-3 is restricted to astrocytes in the rat thalamus. A light and electron-microscopic immunolocalization. Neuroscience 83:815–828.

Errington AC, Renger JJ, Uebele VN, Crunelli V (2010) State-dependent firing determines intrinsic dendritic Ca$^{2+}$ signaling in thalamocortical neurons. J Neurosci 30:14843–14853.

Famiglietti EV Jr, Peters A (1972) The synaptic glomerulus and the intrinsic neuron in the dorsal lateral geniculate nucleus of the cat. J Comp Neurol 144:285–334.

Glykys J, Mody I (2007) The main source of ambient GABA responsible for tonic inhibition in the mouse hippocampus. J Physiol 582:1163–1178.

Godwin DW, Van Horn SC, Eriir A, Sesma M, Romano C, Sherman SM (1996) Ultrastructural localization suggests that retinal and cortical inputs access different metabotropic glutamate receptors in the lateral geniculate nucleus. J Neurosci 16:8181–8192.

Govindaiah, Cox CL (2004) Synaptic activation of metabotropic glutamate receptors regulates dendritic outputs of thalamic interneurons. Neuron 41:611–623.

Govindaiah G, Cox CL (2006) Metabotropic glutamate receptors differentially regulate GABAergic inhibition in thalamus. J Neurosci 26:13443–13453.

Govindaiah G, Cox CL (2009) Distinct roles of metabotropic glutamate receptor activation on inhibitory signalling in the ventral lateral geniculate nucleus. J Neurophysiol 101:1761–1773.

Grossman A, Lieberman AR, Webster KE (1973) A Golgi study of the rat dorsal lateral geniculate nucleus. J Comp Neurol 150:441–466.

Hamos JE, Van Horn SC, Raczkowski D, Uhlrich DJ, Sherman SM (1985) Synaptic connectivity of a local circuit neurone in lateral geniculate nucleus of the cat. Nature 317:618–621.

Harris RM, Hendrickson AE (1987) Local circuit neurons in the rat ventrobasal thalamus—a GABA immunocytochemical study. Neuroscience 21:229–236.

Holdefer RN, Norton TT, Godwin DW (1989) Effects of bicuculline on signal detectability in lateral geniculate relay cells. Brain Res 488:341–347.

Hughes SW, Cope DW, Blethyn KL, Crunelli V (2002) Cellular mechanisms of the slow (<1 Hz) oscillation in thalamocortical neurons in vitro. Neuron 33:947–958.

Jia F, Pignataro L, Schofield CM, Yue M, Harrison NL, Goldstein PA (2005) An extrasynaptic GABA$_A$ receptor mediates tonic inhibition in thalamic VB neurons. J Neurophysiol 94:4491–4501.

Lorincz ML, Kékesi KA, Juhász G, Crunelli V, Hughes SW (2009) Temporal framing of thalamic relay-mode firing by phasic inhibition during the alpha rhythm. Neuron 63:683–696.

McCormick DA, von Krosigk M (1992) Corticothalamic activation modulates thalamic firing through glutamate "metabotropic" receptors. Proc Natl Acad Sci U S A 89:2774–2778.

Ohara PT, Lieberman AR, Hunt SP, Wu JY (1983) Neural elements containing glutamic acid decarboxylase (GAD) in the dorsal lateral geniculate nucleus of the rat: immunohistochemical studies by light and electron microscopy. Neuroscience 8:189–211.

Rossi DJ, Hamann M, Attwell D (2003) Multiple modes of GABAergic inhibition of rat cerebellar granule cells. J Physiol 548:97–110.

Sherman SM (2004) Interneurons and triadic circuitry of the thalamus. Trends Neurosci 27:670–675.

Sillito AM, Kemp JA (1983) The influence of GABAergic inhibitory processes on the receptive field structure of X and Y cells in cat dorsal lateral geniculate nucleus (dLGN). Brain Res 277:63–77.

Sur C, Farrar SJ, Kerby J, Whiting PJ, Atack JR, McKernan RM (1999) Preferential coassembly of α4 and δ subunits of the gamma-aminobutyric acid A receptor in rat thalamus. Mol Pharmacol 56:110–115.

Szentagothai J (1963) The structure of the synapse in the lateral geniculate nucleus. Acta Anat (Basel) 55:166–185.

Wall MJ, Usowicz MM (1997) Development of action potential-dependent and independent spontaneous GABA receptor-mediated currents in granule cells of postnatal rat cerebellum. Eur J Neurosci 9:533–548.

Williams SR, Turner JP, Anderson CM, Crunelli V (1996) Electrophysiological and morphological properties of interneurones in the rat dorsal lateral geniculate nucleus in vitro. J Physiol 490:129–147.

Zhu JJ, Lytton WW, Xue JT, Uhlrich DJ (1999) An intrinsic oscillation in interneurons of the rat lateral geniculate nucleus. J Neurophysiol 81:702–711.